



Energy and exergy study of a hydrogen liquefaction cycle based on liquefied natural gas precooling, and cryocooling using the Joule Brayton cascade cycle

Mehdi Mahboobtosi

Department of Mechanical Engineering, Babol Noshirvani University of Technology, Babol, Iran
Davood Domiri Ganji*

Department of Mechanical Engineering, Babol Noshirvani University of Technology, Babol, Iran
Mofid Gorji

Department of Mechanical Engineering, Babol Noshirvani University of Technology, Babol, Iran

Abstract

The use of hydrogen as a clean fuel has gained the attention of many scientists due to the energy issues and environmental pollution caused by fossil fuels. A key requirement for expanding hydrogen use is the investigation and thermodynamic analysis of the liquefaction cycle, which includes examining various hydrogen liquefaction cycles during pre-cooling and cryogenic cooling. Analyzed cycle is a liquefaction process that utilizes advanced cascade Joule-Brayton (J-B) refrigeration cycles and a dual-pressure organic Rankine cycle, assisted by LNG regasification. Simulations and analyses were conducted using Aspen HYSYS V12. The results showed that in all cycles, over 50% of the input exergy is lost during the cryogenic cooling stage. The value of SEC, COP and EXE cycle is 6.618 kWh/kg_{LH₂}, 0.19884 and 45.797% respectively. Analyzing the energy and exergy of liquefaction cycles is an important step toward improving cycle efficiency, identifying weaknesses, and modifying cycles to enhance performance.

Keywords: Hydrogen liquefaction, LNG, Aspen HYSYS, Hydrogen, Clen fuel

Introduction

Global warming presents a serious threat to human life and development [1]. Since the industrial revolution, the widespread use of fossil fuels has significantly boosted global economic growth and industrialization. However, it has also led to climate change and air pollution on a worldwide scale. Hydrogen, known as a clean fuel [2], has gained considerable attention as an alternative to traditional fuels because it is the most abundant element on Earth, and its combustion produces heat and water (H₂O), which are environmentally friendly [3]. However, transporting and storing hydrogen as a fuel is challenging due to its very low density [4]. Liquefying hydrogen is the most effective way to increase its density and mitigate the issues caused by its low density. Consequently, advancing the hydrogen liquefaction industry will facilitate the adoption of hydrogen energy, reduce fossil fuel consumption, and significantly address concerns about energy supply. James Dewar was the first to successfully liquefy hydrogen in 1898 [5]. In 1904, he and his colleagues constructed the country's first hydrogen liquefier, capable of producing 500–600 cubic feet per hour [6]. The purpose of building a hydrogen liquefaction plant is to produce liquid hydrogen at atmospheric pressure, as it can be supplied to the market at ambient pressure. To achieve this, hydrogen must be cooled from room temperature to its normal boiling point (20.23 K), changing its state from gas to liquid. As previously mentioned, hydrogen gas is liquefied to facilitate long-distance transport, ensuring safety using special low-temperature tanks. The hydrogen liquefaction process is generally divided into four stages [7]: compression, pre-cooling, cryogenic cooling, and liquefaction. hydrogen pressure during pre-compression has minimal effect on pre-cooling, it significantly impacts the cooling curves during cryogenic cooling [7]. When selecting the pre-compression pressure, the efficiency of the cryogenic expansion process and the maximum pressure limit of the heat exchangers should be considered. Hydrogen liquefaction typically requires a feed pressure of 15 to 30 bar [8]. Kuendig et al. [9] proposed a conceptual design for industrial-scale liquid hydrogen production, utilizing liquefied natural gas (LNG) as a precooling system. Their findings suggest that this innovative approach can significantly reduce both operational and initial capital costs in hydrogen liquefaction plants due to the utilization of LNG as a free cooling source. Valenti and Macchi introduced a novel method for hydrogen liquefaction with an efficiency of 48% relative to the Carnot cycle. This method utilizes a helium refrigeration cycle to provide the necessary cooling. High-pressure helium gas undergoes parallel expansion in multiple stages, generating the required temperature for each cooling step. In this process, both hydrogen precooling and cryogenic cooling are integrated within the helium refrigeration cycle [10]. A novel optimized design for a 100 tone/day hydrogen liquefaction plant utilizing a multi-component refrigeration system has been proposed by Krasae-In [11]. This system can be used to cool the normal feed hydrogen gas from 25 °C to the equilibrium temperature of –193 °C. A simplified five-component mixture of refrigerant is suggested for the plant. Pressure drops in the heat exchangers are also employed in the study simulation, but the results show that they



do not have a significant impact on the overall plant total power consumption. A novel and efficient hydrogen liquefaction process has been analyzed by Sadaghiani et al. [12]. This process utilizes two independent refrigeration cycles with different mixed refrigerants and is capable of producing 300 tons of liquid hydrogen per day. In this process, hydrogen gas at 25 °C and 21bar, with a flow rate of 3.450 kg/s, is cooled and liquefied to the equilibrium temperature (-195 °C) by the first refrigeration cycle. The energy consumption of this cycle is 1.102 kWh/kg_{LH2}. In the second refrigeration cycle, the hydrogen is cooled to -253 °C with a power consumption of 3.258 kWh/kg_{LH2}. This process boasts the least total power consumption compared to similar liquefaction plants. The thermal design of heat exchangers and expanders over a wide temperature range, along with the use of innovative and appropriate mixed refrigerants according to the configuration, are novel aspects of this process. Additionally, the composition of the first and second refrigeration cycles' refrigerants is another innovation. The study also includes energy and exergy analyses of the proposed process. The coefficient of performance (COP) of the process is 0.1797, which is considerably higher than other comparable processes. An innovative and efficient large-scale hydrogen liquefaction process has been proposed by Riaz et al. [13]. In this complex and energy-intensive process, the cold energy of LNG is utilized in the precooling stage. The results showed that a para-hydrogen concentration of more than 99.5% is achieved with a total specific energy consumption of 7.64 kWh/kg_{LH2} and an exergy efficiency of 42.25%. Due to its simplicity and effective utilization of LNG cold energy, the proposed process outperforms previous industrial and reported processes, offering approximately 43.7% energy savings. Chang et al. [14] examined the efficiency of the hydrogen liquefaction cycle using a helium cooling cycle. In their study, the pre-cooling stage utilized a liquefied natural gas recovery system. They investigated two operating pressures, 100 and 7000 kPa, in the LNG recovery system. The results showed that the hydrogen liquefaction cycle was more efficient when the operating pressure in the LNG line was reduced. Yang et al.'s [15] study explored three different methods for hydrogen precooling: a cascade precooler that utilized both LNG and LN₂, and two separate precoolers using LNG and LN₂ individually. The study found that the SEC for liquefaction decreased from 13.58 to 11.05 kWh/kg_{LH2}. The results indicated that the cascade precooler had the most efficient configuration. Bi et al. [16] introduced a cycle in a hydrogen liquefier that uses cascade precooling with LNG and LN₂. Cho et al. [17] used a mixed refrigerant (MR) in the precooling stage with LNG, reducing the SEC from 4.36 to 4.07 kWh/kg_{LH2}. To decrease energy consumption in the hydrogen liquefaction process, Ghorbani et al. [18] developed an LNG gasification method for hydrogen precooling. Their findings showed that the integrated system's SEC and coefficient of performance (COP) were 4.772 kWh/kg_{LH2} and 0.175, respectively. This research investigates a hydrogen liquefaction cycle. Thermodynamic analysis, exergy analysis, SEC, COP, and EXE of the liquefaction cycle are examined. The cycle is a liquefaction process that utilizes advanced cascade Joule-Brayton (J-B) refrigeration cycles and a dual-pressure organic Rankine cycle, assisted by LNG regasification. In this hydrogen cycle, the feed is pre-cooled by liquefied natural gas. It is then chilled and liquefied through cascade Joule-Brayton cycles. Ultimately, liquid hydrogen is produced that meets the pressure and parahydrogen conditions. The proposed cycles are modeled in Aspen HYSYS V12.1, a process simulator that combines thermodynamics, engineering techniques, and numerical calculations.

Process simulation

Figure 1 illustrates the diagram for the liquefaction cycle, which integrates dual-pressure organic Rankine cycle, LNG, and helium cascade cooling. In this cycle, LNG cold energy is used to pre-cool hydrogen and also powers the dual-pressure organic Rankine cycle to generate electricity. A pump (P-2) increases the LNG pressure to 3000 kPa, and it is then used to pre-cool hydrogen, which heats itself (streams L6, L7) to the regasification temperature (10°C). HX2 divides the LNG into two streams (L3, L4). Stream L4 acts as the cold sink for the dual-pressure organic Rankine cycle, while the other stream goes into HX1 to pre-cool hydrogen directly. In the dual-pressure organic Rankine cycle, condensed working fluid enters HX1 to pre-cool hydrogen. However, the working fluid isn't heated to the correct temperature in HX1, so it is sent to H-1, which uses seawater. The working fluid expands in E-1 and generates electricity during regasification. A gas and liquid separator (S-1) is used to separate the two phases formed during the initial expansion. While R5 enters HX3 and is condensed by LNG, R11 undergoes further expansion in E-2 before entering HX3. To pump two liquid streams simultaneously, R8's pressure is reduced via a pressure relief valve and combined with R13 (both streams have equal pressure). This cycle incorporates a dual-pressure J-B refrigeration cycle for the hydrogen cryocooling system. Helium is first compressed in the refrigeration cycle using compressors and coolers. It then splits into two streams, undergoing two cascade J-B cycles, Streams 8 and 15. Helium expands in E-3 and E-4 in the first Joule-Brayton cycle, cooling hydrogen. After initial expansion in expander 5, helium in the second Joule-Brayton cycle splits into streams 18 and 21. Stream 18 is further expanded in expander 7 after hydrogen is liquefied in HX-8, while Stream 21 is used to sub-cool liquid hydrogen following the second expansion. At the HX8 intake, streams 20 and 23 eventually merge. The enhanced cycle achieves higher helium utilization efficiency compared to the dual-pressure Joule-Brayton cycle. R41 is used as the working fluid in dual-pressure organic Rankine cycle. The efficiency and specifications of the equipment used, along with the input and output conditions for hydrogen and LNG, are detailed in Table 1. The following assumptions are made to effectively simulate and evaluate the proposed process:

- Pressure losses in the heat exchanger, heater, and cooler are not considered.
- Disregarding the impacts of potential and kinetic energy, the proposed liquefaction process is considered to be in a steady state.



- The pressure ratios of the compressors in the proposed cycle are equal and less than three to reduce power consumption.
- The energy losses in separators and mixers are not considered.

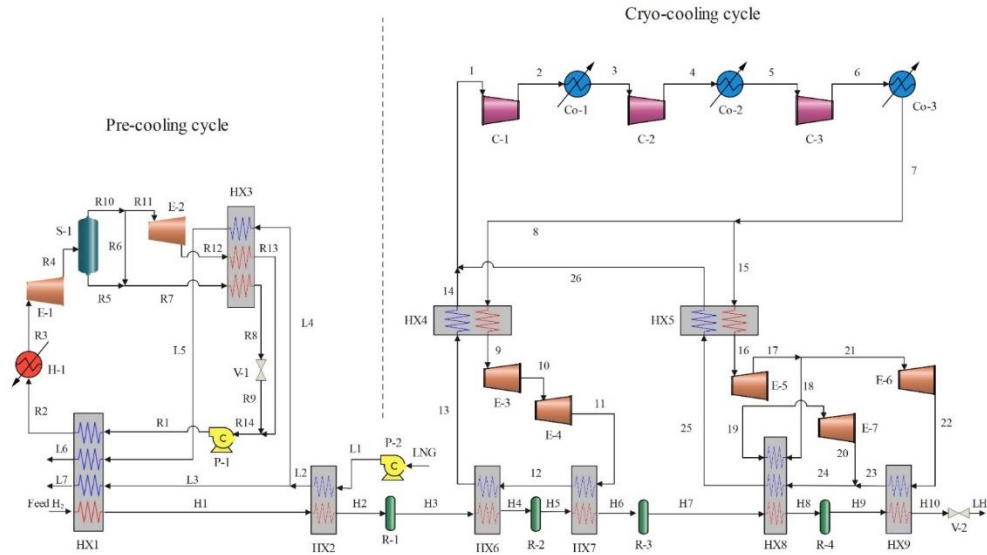


Figure (1) Diagram of the liquefaction cycle

Table 1- Information about cycle

Parameter	Value	Unit
Equipment condition		
Adiabatic efficiency of pump	75	%
Isentropic efficiency of compressor	80	%
Isentropic efficiency of expander	85	%
Feed hydrogen condition		
Temperature	25	°C
Pressure	2100	kpa
Para-hydrogen proportion	25	%
Product condition		
Product capacity	120	TPD
Temperature	21	K
Pressure	130	kpa
Para-hydrogen ratio	>95	%
LNG parameter		
Temperature	-160	°C
Pressure	120	kpa
Components of LNG		Mole %
Nitrogen	0.2	
Methane	91.3	
Ethane	5.4	
Propane	2.1	
i-Butane	0.5	
n-Butane	0.5	

Formulation

The energy and exergy equations are essential for the thermodynamic analysis of chemical equipment. The equipment studied can be categorized as an open system under steady-state flow conditions. Therefore, as shown in Table 2, the equipment in these cycle is appropriate for energy and exergy calculations. To evaluate the performance of each piece of equipment, exergy efficiency is calculated along with the exergy equations. There are two methods for calculating exergy efficiency: consumption-production efficiency and input-output efficiency. In the cycle reviews, the first

method is applied. It is important to note that exergy efficiency calculations for inefficient equipment are not considered. The formulas for determining the energy efficiency of various equipment are provided in Table 3.

Table 2- Equipment energy and exergy equations

Equipment	Energy equation	Exergy equation
Compressor	$\dot{W}_C = \dot{m}_C(h_{out} - h_{in})$	$\dot{I}_C = \dot{W}_C - \dot{m}_C(e_{out} - e_{in})$
Expander	$\dot{W}_E = \dot{m}_E(h_{in} - h_{out})$	$\dot{I}_E = \dot{m}_E(e_{in} - e_{out}) - \dot{W}_E$
Pump	$\dot{W}_P = \dot{m}_P(h_{out} - h_{in})$	$\dot{I}_P = \dot{W}_P - \dot{m}_P(e_{out} - e_{in})$
Valve	$h_{V,in} = h_{V,out}$	$\dot{I}_V = \dot{m}_V(e_{in} - e_{out})$
Heat exchanger	$\sum \dot{m}_h(h_{in} - h_{out})_h = \sum \dot{m}_c(h_{out} - h_{in})_c$	$\dot{I}_{HX} = \sum \dot{m}_{HX}(e_{in} - e_{out})$
Cooler	$\dot{Q}_{Co} = \dot{m}_{Co}(h_{in} - h_{out})$	$\dot{I}_{Co} = \dot{m}_{Co}(e_{in} - e_{out})$
Heater	$\dot{Q}_H = \dot{m}_H(h_{out} - h_{in})$	$\dot{I}_H = \dot{m}_H(e_{in} - e_{out})$

Table 3- Exergy efficiency of equipment

Equipment	Exergy efficiency
Compressor	$\varepsilon_C = \frac{\dot{m}_C(e_{out} - e_{in})}{\dot{W}_C}$
Expander	$\varepsilon_E = \frac{\dot{m}_E(e_{in} - e_{out})}{\dot{W}_E}$
Pump	$\varepsilon_P = \frac{\dot{m}_P(e_{out} - e_{in})}{\dot{W}_P}$
Heat exchanger	$\varepsilon_{HX} = \frac{\sum \dot{m}_h(e_{out} - e_{in})_h}{\sum \dot{m}_c(e_{in} - e_{out})_c}$

The energy used in the cycle includes both the power provided by the surrounding environment and the output power from the expander. Equation (1) shows the total power needed for the liquefaction cycle, assuming that the energy-consuming equipment can fully use the expander's power output without any losses.

$$\dot{W}_{net} = \sum \dot{W}_{C-i} + \sum \dot{W}_{P-i} - \sum \dot{W}_{E-i} \quad (1)$$

SEC is a shorthand the specific energy consumption to liquefy hydrogen. It is a key parameter, calculated using equation (2), to assess the performance of the cycle.

$$SEC = \frac{\dot{W}_{net}}{\dot{m}_{LH_2}} \quad (2)$$

Also, the following relationship can be used to analyze the way of distribution and application of input exergy:

$$\sum \dot{W}_C + \sum \dot{W}_P + \Delta \dot{E}_{LNG} = \Delta \dot{E}_{H_2} + \sum \dot{W}_E + \sum \dot{I} \quad (3)$$

The system's coefficient of performance (COP) and exergy efficiency (EXE) were used to assess the thermodynamic efficiency of the cycle. The relationships related to these two parameters are given in relation 4 and 5.

$$COP = \frac{\dot{m}_{LH_2}(h_{Feed} - h_{LH_2})}{\dot{W}_{net}} \quad (4)$$

$$EXE = \frac{\dot{W}_{min}}{\dot{W}_{net}} = \frac{\dot{m}_{LH_2}(e_{LH_2} - e_{Feed})}{\dot{W}_{net}} \quad (5)$$

Hydrogen can exist as either ortho or para forms, depending on the spin orientation of the nuclei. In para hydrogen molecules, the spin of one atom is opposite to that of the other, with one spinning counterclockwise and the other clockwise. Conversely, in ortho hydrogen molecules, both atoms have parallel spin orientations, both spinning clockwise. Para hydrogen is more stable at lower temperatures and has lower energy, whereas ortho hydrogen is more excited and has higher energy levels. The conversion rate is adjusted during the simulation by modifying the conversion coefficients, as demonstrated by the following formula:

$$Conversion(\%) = C_0 + C_1T + C_2T^2 \quad (6)$$

Results Discussion

Table 4 details the streams in the third cycle, including all necessary information for a thermodynamic analysis of the cycle and its equipment. The table also displays the percentage of hydrogen para, indicating that the cycle meets the required hydrogen para levels. Figures 2a–2i show the relationship between temperature, heat flow, LMTD, minimum approach, and temperature differences for each heat exchanger in Cycle. The helium self-cooling heat exchangers (HX4-HX5) in this cycle have a minimum approach of approximately 2°C, a crucial factor for enhancing cryocooling efficiency.

Table 4- Cycle stream information



Stream ID	Temperature T (°C)	Pressure p (kPa)	Mass flow \dot{m} (TPD)	Para (%)	Mass enthalpy h (kJ/kg)	Mass entropy s (kJ/kg-°C)	Mass exergy e (kJ/kg)
Feed H ₂	25	2100	120	25	5.84	54.29	3735.79
H1	-94.22	2100	120	25	-1713.11	46.92	4213.41
H2	-156.02	2100	120	25	-2620.33	40.69	5163.39
H3	-154.93	2100	120	33.62	-2620.35	42.24	5149.88
H4	-199.98	2100	120	33.62	-3316.35	34.8	6673.28
H5	-197.02	2100	120	51.61	-3316.39	37.82	6582.7
H6	-227	2100	120	51.61	-3853.7	28.71	8760.42
H7	-223.09	2100	120	77.62	-3853.76	32.68	8452.82
H8	-242.01	2100	120	77.62	-4434.23	17.66	12351.6
H9	-239.97	2100	120	95.52	-4434.28	20.08	11941.1
H10	-252.54	2100	120	95.52	-4731.42	8.93	14967.1
LH ₂	-252.16	130	120	95.52	-4731.42	10	14646.6
LNG	-160	120	520.8		-5167.14	4.29	957.9
L1	-158.46	3000	520.8		-5158.72	4.31	959.01
L2	-99.01	3000	520.8		-4949.68	5.76	734.92
L3	-99.01	3000	80.9		-4949.68	5.76	734.92
L4	-99.01	3000	439.9		-4949.68	5.76	734.92
L5	-6610	3000	439.9		-4586.93	7.71	518.29
L6	10	3000	439.9		-4358.97	8.67	461.05
L7	10	3000	80.9		-4358.97	8.67	461.05
R1	-96.5	2831.9	364.9		-7504.08	-0.25	315.14
R2	-20.5	2831.9	364.9		-7344.65	0.5	252.67
R3	10	2831.9	364.9		-6958.29	1.88	226.97
R4	-65.1	219.2	364.9		-7053.35	1.96	107.87
R5	-65.1	219.2	62.52		-7445.11	0.01	277.52
R6	-65.1	219.2	64.98		-6972.35	2.35	72.79
R7	-65.1	219.2	127.5		-7204.16	1.23	173.18
R8	-97.5	-127.5	127.5		-7508.06	-0.25	312.5
R9	-97.45	110.4	127.5		-7508.06	-0.25	312.27
R10	-65.1	219.2	302.4		-6972.35	2.35	72.79
R11	-65.1	219.2	237.4		-6972.35	2.35	72.79
R12	-78.6	110.4	237.4		-6999.31	2.37	38.54
R13	-97.57	110.4	237.4		-7508.27	-0.25	312.42
R14	-97.53	110.4	364.9		-7508.2	-0.25	312.37
1	23	110	1229.3		-10.47	20.81	50.91
2	187.08	275.4	1229.3		842.07	21.19	788.85
3	25	275.4	1229.3		-0.2	18.93	619.22
4	190.2	689.5	1229.3		858.2	19.32	1363.01
5	25	689.2	1229.3		-0.48	17.03	1187.6
6	190.23	1726.3	1229.3		858.21	17.41	1931.65
7	25	1726.3	1229.3		-1.14	15.12	1756.09
8	25	1726.3	455		-1.14	15.12	1756.09
9	-163.1	1726.3	455		-981.66	9.92	2325.39
10	-202.87	435.8	455		-1185.76	10.46	1960.47
11	-228.23	110	455		-1316.41	11	1668.88
12	-201	110	455		-1174.7	13.47	1075.17
13	-165.7	110	455		-991.14	15.54	641.23
14	22.97	110	455		-10.63	20.8	50.91
15	25	1726.3	774.3		-1.14	15.12	1756.09
16	-225.1	1726.3	774.3		-1308.92	5.54	3304.85
17	-246.6	279.3	774.3		-1414.01	6.29	2976.25
18	-246.6	279.3	238.4		-1414.01	6.29	2976.25

19	-231.1	279.3	238.4	-1332.52	8.71	2336.47
20	-241	110	238.4	-1383.03	9.25	2122.37
21	-246.6	279.3	535.9	-1414.01	6.29	2976.25
22	-253.71	110	535.9	-1449.56	6.62	2841.37
23	-241	110	535.9	-1383.03	9.25	2122.37
24	-241	110	774.3	-1383.03	9.25	2122.37
25	-228.56	110	774.3	-1318.16	10.96	1678.79
26	23.02	110	774.3	-10.38	20.81	50.91

Figure 3a presents the exergy loss rates of various equipment parts in the pre-cooling process. HX1 exhibits the highest exergy loss rate (24.55%) due to heat transfer inefficiencies. Generally, significant exergy losses are observed in heat exchangers (HX1, HX3) and heaters/evaporators (H-1, E-1). Figure 3b illustrates the distribution of input exergy into exergy losses, recoverd work, and useful exergy for pre-cooling, with HX2 having the highest useful exergy ratio, indicating efficient heat transfer, likely due to optimal operating conditions. Figure 3c shows exergy loss rates in cryocooling equipment, where coolers (Co-1, Co-2, Co-3) exhibit the highest exergy losses (13.02%, 13.01%, and 12.58%). Among heat exchangers (HX5, HX6, HX7, HX8, HX9), HX5 and HX8 have higher exergy losses (3.7% and 1.7%, respectively), potentially due to temperature gradients or heat transfer surface inefficiencies, while HX6, HX7, and HX9 have lower losses, indicating better performance or lighter load conditions. Among expanders (E-3, E-4, E-5, E-6, E-7), E-5 has a significant exergy loss rate of 10.44%, whereas E-3 and E-4 have about 4.4%, indicating moderate inefficiencies. E-6 and E-7 show lower losses, reflecting better operational conditions. Compressors exhibit an exergy loss rate of 8.5%, possibly due to high condensation temperatures causing significant irreversibility. Figure 3d displays how input exergy is utilized in the cryocooling section, with over half of it allocated to exergy losses.

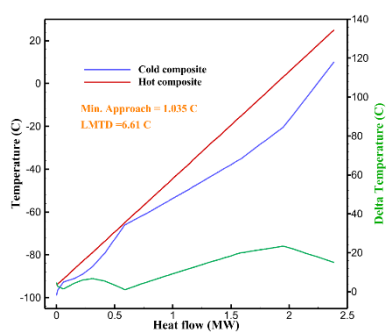


Figure (2a) HX1 information

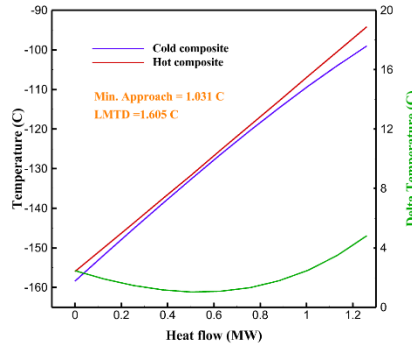


Figure (2b) HX2 information

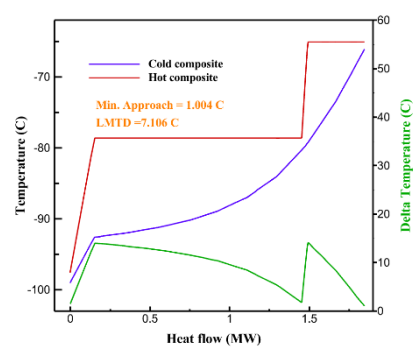


Figure (2c) HX3 information

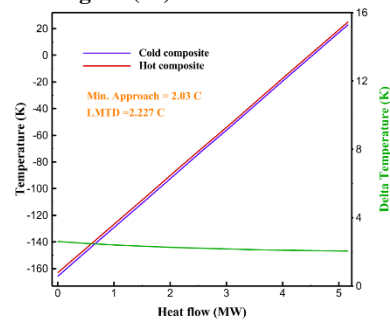


Figure (2d) HX4 information

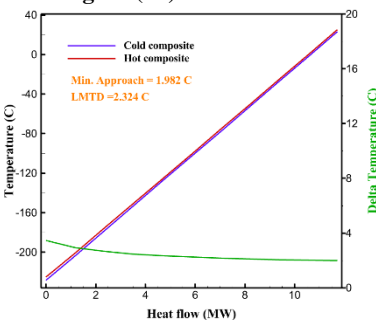


Figure (2e) HX5 information

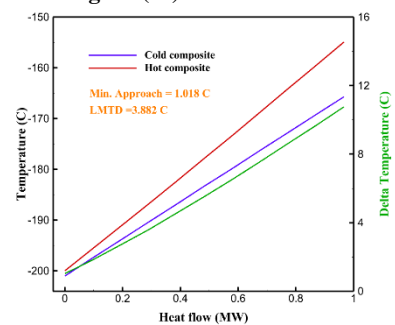


Figure (2f) HX6 information

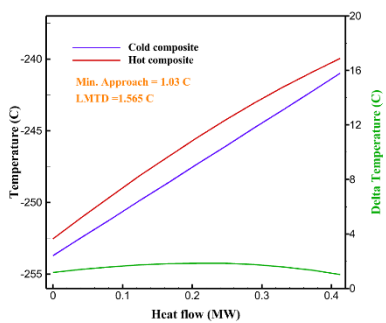
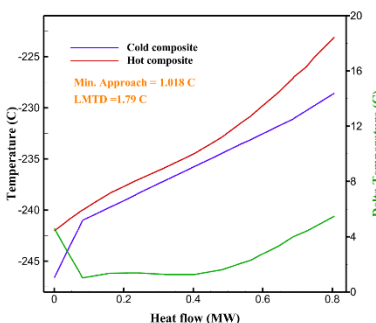
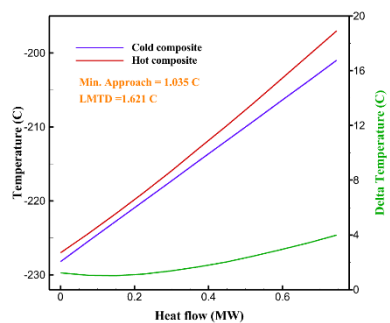




Figure (2g) HX7 information

Figure (2h) HX8 information

Figure (2i) HX9 information

Figure 3e provides the exact exergy loss in kW for all cycle equipment, while Figure 3f shows exergy efficiency, with HX2 achieving the highest efficiency. High exergy efficiency indicates effective energy conversion into useful work, leading to better energy utilization, reduced waste, and improved overall process efficiency. Identifying and optimizing equipment with low exergy efficiency can significantly lower operating costs by requiring less input energy for the same output. Overall, focusing on exergy efficiency helps improve energy use, reduces costs, boosts system performance, and supports ongoing optimization in hydrogen liquefaction processes. Table 5 outlines the power of the cycle components.

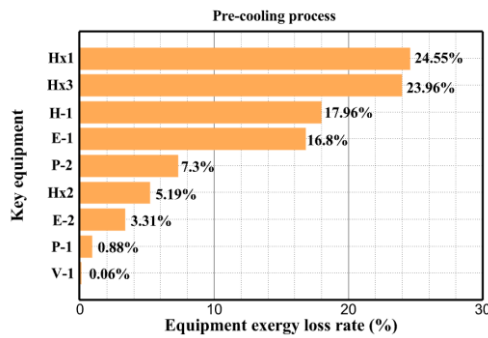


Figure (3a) Equipment exergy loss rate in pre-cooling process

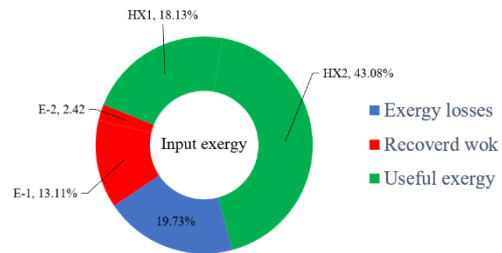


Figure (3b) Use of input exergy in pre-cooling process

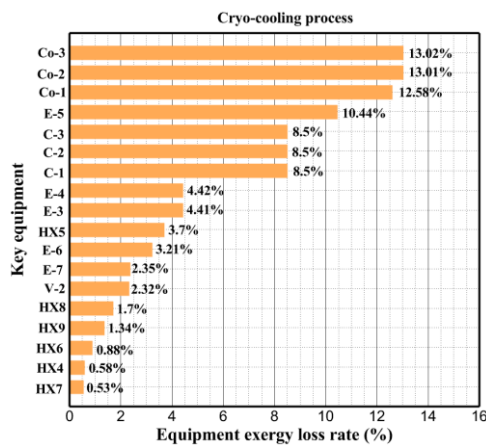


Figure (3c) Equipment exergy loss rate in cryo-cooling process

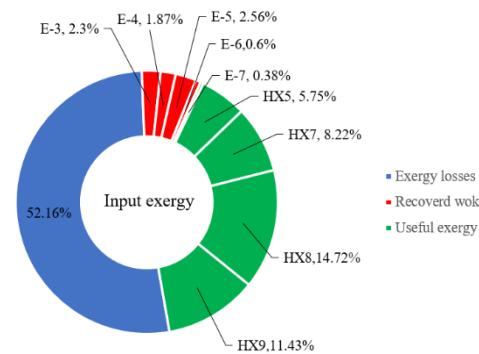


Figure (3d) Use of input exergy in cryo-cooling process

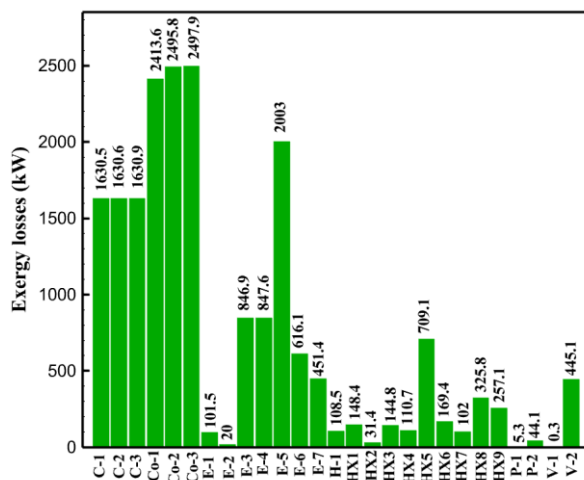


Figure (3e) Exergy losses each equipment cycle

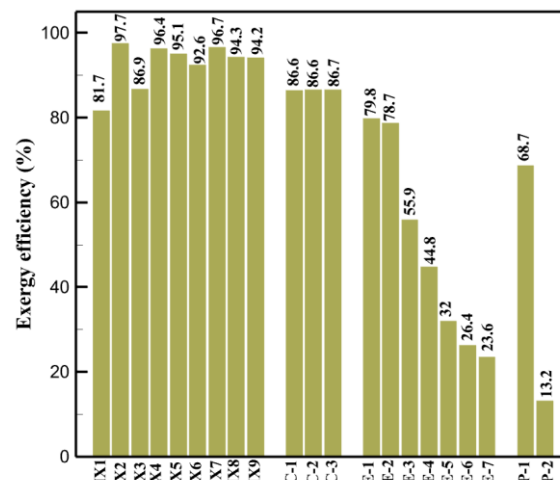


Figure (3f) Exergy efficiency of equipment cycle

Table 5- Equipment power cycle

Equipment	Power (kW)
-----------	------------



Comps	C-1	12130
	C-2	12213.3
	C-3	12217.4
Exps	E-1	401.48
	E-2	74.08
	E-3	1074.87
	E-4	688.02
	E-5	941.83
	E-6	220.5
	E-7	139.36
Pumps	P-1	17.04
	P-2	50.79

Conclusions

This study conducted a thermodynamic analysis of hydrogen liquefaction cycles. The cycle is a liquefaction process that utilizes advanced cascade Joule-Brayton (J-B) refrigeration cycles and a dual-pressure organic Rankine cycle, assisted by LNG regasification. Some of the findings of the research are given below:

- In liquefaction cycles, the cooler positioned after the final compressor experiences the highest amount of exergy losses.
- In the cycle, over 50% of the input exergy is lost as exergy losses during the cryocooling stage.
- In the cycle, HX2 has the highest exergy efficiency, while the LNG pump has the lowest.
- The thermodynamic analysis of the cycle revealed that the compressors consume the most power. Among them, Compressor C-3 requires the greatest amount of power.

The value of SEC, COP and EXE cycle is 6.618 kWh/kg_{LH2}, 0.19884 and 45.797% respectively.

List of Symbols

The list of symbols comes after the acknowledgment and before references. The English symbols come first followed by the Greek symbols. Both must be typed in alphabetical order and separated.

Subscripts		s	mass entropy
E	expander	ε	exergy efficiency
Co	cooler	p	pressure
C	compressor	T	temperature
Ev	evaporator	\dot{W}	work rate
H	heater	\dot{Q}	heat rate
HX	heat exchanger	Acronyms	
i	equipment number	COP	coefficient of performance
in	inlet stream	EXE	exergy efficiency of the system
out	outlet stream	J-B	Joule-Brayton
c	cold stream	MR	mixed refrigerant
h	hot stream		
net	net power	N ₂	nitrogen
S	separator	LH ₂	liquid hydrogen
R	reactor	LMTD	logarithmic mean temperature difference
P	pump	LN ₂	liquid nitrogen
V	valve	LNG	liquefied natural gas
Nomenclature		ORC	organic Rankine cycle
\dot{E}	exergy rate	SEC	specific energy consumption
e	mass exergy	TPD	tons per day
\dot{I}	exergy loss rate		
h	mass enthalpy		
\dot{m}	mass flow rate		

References

- [1] Mazloomi K, Gomes C. Hydrogen as an energy carrier: Prospects and challenges. *Renew Sust Energy Rev* 2012;16(5):3024–33.
- [2] Yang Y, Tong L, Yin S, Liu Y, Wang L, Qiu Y, et al. Status and challenges of applications and industry chain technologies of hydrogen in the context of carbon neutrality. *J Clean Prod* 2022;376:134347.
- [3] Bae J-E, Wilailak S, Yang J-H, Yun D-Y, Zahid U, Lee C J. Multi-objective optimization of hydrogen liquefaction process integrated with liquefied natural gas system. *Energy Convers Manage* 2021;231:113835.



- [4] Wietschel M, Ball M. The hydrogen economy: opportunities and challenges. Cambridge University Press; 2009
- [5] J. Dewar, Liquid hydrogen: preliminary note on the liquefaction of hydrogen and helium, *Science* 8 (1898) 3–6.
- [6] B.A. Hands, The first hydrogen liquefier in the USA, *AIP Conf. Proc.* 710 (2004) 255–263.
- [7] Walnum, H. T., Berstad, D., Drescher, M., Neksa, P., Quack, H., Haberstroh, C., & Essler, J. (2012). Principles for the liquefaction of hydrogen with emphasis on precooling processes. *12th Cryogenics*, 2012, 8.
- [8] Cardella U, Decker L, Klein H. Roadmap to economically viable hydrogen liquefaction. *Int J Hydrogen Energy* 2017;42(19):13329–38.
- [9] Kuendig A, Loehlein K, Kramer GJ, Huijsmans J. Large scale hydrogen liquefaction in combination with LNG re-gasification. *16th World Hydrogen Energy. Conference 2006*
- [10] Valenti, G., & Macchi, E. (2008). Proposal of an innovative, high-efficiency, large-scale hydrogen liquefier. *International journal of hydrogen energy*, 33(12), 3116-3121.
- [11] Krasae-In, S. (2014). Optimal operation of a large-scale liquid hydrogen plant utilizing mixed fluid refrigeration system. *International journal of hydrogen energy*, 39(13), 7015-7029.
- [12] Sadaghiani, M. S., & Mehrpooya, M. (2017). Introducing and energy analysis of a novel cryogenic hydrogen liquefaction process configuration. *International journal of hydrogen energy*, 42(9), 6033-6050.
- [13] Riaz, A., Qyyum, M. A., Min, S., Lee, S., & Lee, M. (2021). Performance improvement potential of harnessing LNG regasification for hydrogen liquefaction process: Energy and exergy perspectives. *Applied Energy*, 301, 117471.
- [14] Chang, H. M., Kim, B. H., & Choi, B. (2020). Hydrogen liquefaction process with Brayton refrigeration cycle to utilize the cold energy of LNG. *Cryogenics*, 108, 103093.
- [15] Yang, Y., Park, T., Kwon, D., Jin, L., & Jeong, S. (2020). Effectiveness analysis of pre-cooling methods on hydrogen liquefaction process. *Progress in Superconductivity and Cryogenics*, 22(3), 20-24.
- [16] Bi, Y., & Ju, Y. (2022). Design and analysis of an efficient hydrogen liquefaction process based on helium reverse Brayton cycle integrating with steam methane reforming and liquefied natural gas cold energy utilization. *Energy*, 252, 124047.
- [17] Cho, S., Park, J., Noh, W., Lee, I., & Moon, I. (2021). Developed hydrogen liquefaction process using liquefied natural gas cold energy: Design, energy optimization, and techno-economic feasibility. *International Journal of Energy Research*, 45(10), 14745-14760.
- [18] Ghorbani, B., Zendehboudi, S., & Jouybari, A. K. (2022). Thermo-economic optimization of a hydrogen storage structure using liquid natural gas regasification and molten carbonate fuel cell. *Journal of Energy Storage*, 52, 104722.